High-strength, thermal-insulating, fire-safe bio-based organic lightweight aerogel based on 3D network construction of natural tubular fibers

Yue Xu, Chentao Yan, Chunlin Du, Kai Xu, Yixuan Li, Miaojun Xu, Serge Bourbigot, Gaelle Fontaine, Bin Li, Lubin Liu

High-strength, thermal-insulating, fire-safe bio-based organic lightweight aerogel based on 3D network construction of natural tubular fibers

Yue Xu, Chentao Yan, Chunlin Du, Kai Xu, Yixuan Li, Miaojun Xu, Serge Bourbigot, Gaelle Fontaine, Bin Li, Lubin Liu

PII: S1359-8368(23)00312-8

DOI: https://doi.org/10.1016/j.compositesb.2023.110809

Reference: JCOMB 110809

To appear in: *Composites Part B*

Received Date: 21 March 2023

Revised Date: 2 May 2023

Accepted Date: 16 May 2023

Please cite this article as: Xu Y, Yan C, Du C, Xu K, Li Y, Xu M, Bourbigot S, Fontaine G, Li B, Liu L, High-strength, thermal-insulating, fire-safe bio-based organic lightweight aerogel based on 3D network construction of natural tubular fibers, *Composites Part B* (2023), doi: https://doi.org/10.1016/j.compositesb.2023.110809.

Graphical Abstract

Title of the manuscript: High-strength, thermal-insulating, fire-safe bio-based organic lightweight aerogel based on 3D network construction of natural tubular fibers

Authors: Yue Xu, Chentao Yan, Chunlin Du, Kai Xu, Yixuan Li, Miaojun Xu*, Serge Bourbigot, Gaelle Fontaine, Bin Li, Lubin Liu*

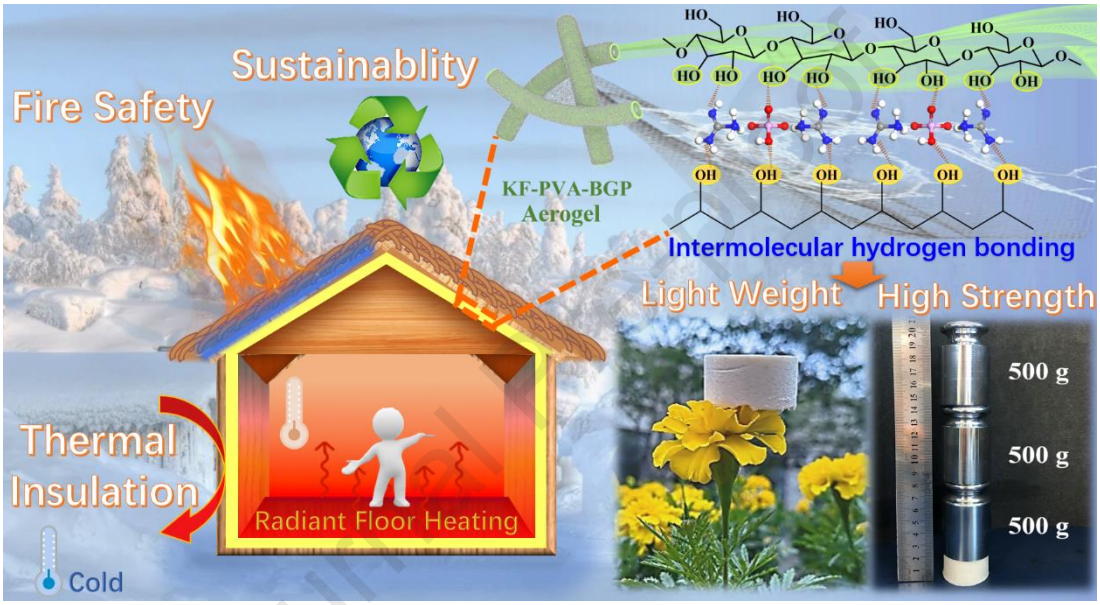

High-strength, thermal-insulating, fire-safe bio-based organic lightweight aerogel based on 3D network construction of natural tubular fibers

Yue Xu[a,b,c,1], Chentao Yan[b,c,1], Chunlin Du[b,c,1], Kai Xu[b,c], Yixuan Li[b], Miaojun Xu[a,b,c,*], Serge Bourbigot[d,e], Gaelle Fontaine[d], Bin Li[a,b,c], Lubin Liu[b,c,*]

[a] *Key Laboratory of Bio-based Material Science and Technology, Ministry of Education, Northeast Forestry University, Harbin 150040, China.*

[b] *Heilongjiang Key Laboratory of Molecular Design and Preparation of Flame Retarded Materials, College of Chemistry, Chemical Engineering and Resource Utilization, Northeast Forestry University, Harbin 150040, China*

[c] *Key Laboratory of Forest Plant Ecology, Ministry of Education, Northeast Forestry University, Harbin 150040, China*

[d] *Univ. Lille, CNRS, INRAE, Centrale Lille Institut, UMR 8207 - UMET - Unité Matériaux et Transformations, F-59000 Lille, France*

[e] *Institut Universitaire de France, Paris, France*

* Corresponding author: Lubin Liu, Miaojun Xu, E-mail: liulubin@nefu.edu.cn, xumiaojun@nefu.edu.cn, Fax number: +86-451-82192699.

[1] These authors contributed to this work equally.

ABSTRACT

Petrochemical-based foam materials are extensively used in insulation and energy storage fields. However, their non-degradability and high flammability have caused great pressure on energy, environment and human life and property safety. It is urgent to carry out research on biodegradable and fire safety alternative biomaterials. Herein, inspired by the natural hollow insulation animal hair, the 3D network structure of tubular aerogel was constructed by using the hollow kapok fibers (KF), the binder polyvinyl alcohol (PVA) and the flame retardant crosslinker biguanide phosphonate (BGP). The multifunctional tubular aerogel integrating thermal insulation, high strength and fire safety was successfully prepared by freeze-forming and freeze-drying. Due to the intermolecular hydrogen bonding and the high viscosity of binder, KF

maintained a high filling, full component and high value utilization. Compared to pure KF, the thermal conductivity of KF-PVA-BGP aerogel was reduced to 0.0531 $W \cdot m^{-1}K^{-1}$ and its compressive strength was improved to 1.64 MPa. Meanwhile, the incorporation of flame retardant cross-linker BGP promoted the degradation and charring of KF-PVA aerogel and released lots of inert gases during decomposition process, which effectively exerted the flame retardant effect in condensed and gas phases. Besides, compared with commercial PS insulation boards, KF-PVA-BGP composites are recyclable, sustainable and biodegradable in addition to their excellent thermal insulation and fire safety performance. This KF-PVA-BGP aerogel showed good application prospects for replacing traditional petrochemical-based materials in thermal insulation, energy storage and new energy fields.

Keywords: Bio-based tubular aerogel; 3D network structure; Thermal insulation; Fire safety; High strength

1. Introduction

In modern society, the demand (≈23 billion square meters in 2022 alone) for building insulation, energy storage and sound absorption materials is growing exponentially every year [1-3]. Organic insulation materials are widely used in the fields of insulation and energy storage due to their advantages of light weight, low thermal conductivity and easy molding [4-6]. Nevertheless, the traditional organic insulation materials are from petrochemical-based materials such as extruded polystyrene board, foamed polystyrene board, polyurethane foam, and their high energy consumption and non-degradation in the production and processing process bringing huge energy and environmental pressure to society [7]. Meanwhile, the traditional organic insulation materials are often flammable and release a large number of toxic gases during combustion process, causing a lot of economic losses (direct loss of 5.85 billion in 2022 of China) and casualties to human beings [8]. Therefore, the development of biodegradable, fire-safe, recyclable bio-based organic insulation materials in line with current sustainable development strategies has become a top priority today.

With the proposal of the dual carbon strategy, a potential and sustainable solution is offered through environmentally friendly and abundant natural products as

substitutes to petroleum-based insulation materials. Hence, bio-based raw materials such as cellulose [9], lignin [10], alginate [11], and chitosan [12] were used to prepared sustainable organic insulation materials, which showed great promise in replacing petrochemical-based insulation materials with similar properties. Among these biomaterials, cellulose, as a bio-based raw materials with the largest reserves on earth, is the most promising alternative material, and it has been widely used in insulation, adsorption, energy storage, electronic and electrical fields [13-16]. Nevertheless, with the continuous development of high-end manufacturing, cellulose-based materials still face numerous challenges in structural construction and multifunctionalization. Usually, the structure of materials decides their performance, and the natural tubular structure affects its insulation properties in nature, such as the feathers of birds and the hair of polar bears, etc. Previous studies on aerogel materials have shown that the construction of tubular structures was beneficial to the thermal insulation of materials [17,18]. However, the traditional preparation methods for cellulose-based tubular aerogels, such as the template method and the introduction of inorganic tubular materials, are more complicated and have a greater impact on the comprehensive performance of materials [19]. Therefore, it is a new way to search a natural, recyclable and sustainable tubular bio-based raw material as a substrate for cellulose-based aerogels. Kapok fibers (KF), as a natural hollow tubular structure with light weight, renewable, degradable and superior biocompatibility, is commonly used in textile, adsorption, solar steam generation and sound insulation fields [20-23]. Meanwhile, KF possessed a low thermal conductivity due to its own tubular structure and can be designed for the construction of tubular bio-based insulation aerogel after surface treatment.

Although natural tubular bio-based aerogels have been constructed using the hollow structure of kapok, the poor fire safety and compression strength of KF aerogels still constrained their application in insulation and energy storage fields due to their own structural composition (64% cellulose and 13% lignin) in practical applications. In the past few years, scholars have conducted a lot of research on flame retardant cellulose-based aerogels [24]. The introduction of inorganic fillers or intumescent flame retardants are the most commonly used modification methods [25]. Among them, the inorganic fillers for flame retardant cellulose-based aerogels mainly included metal hydroxide [26], montmorillonite [27], hydroxyapatite [28] and nano clay [29]. However, the incorporation of inorganic fillers usually decreased the strength and thermal

insulation properties of aerogel composites and increased their density of the materials. Compared with inorganic fillers, intumescent flame retardants exhibited higher flame retardant efficiency in cellulose-based aerogels [30]. But the addition of intumescent flame retardants still cannot give aerogel composites high strength, low density and thermal conductivity while obtaining excellent fire safety properties. Therefore, it is urgent to develop a bio-based aerogel composite with excellent fire safety, light weight, thermal insulation, high strength and biodegradability to meet the needs of practical applications.

Herein, the 3D network construction of KF tubular structure by biodegradable binder PVA and biguanide phosphonate (BGP) significantly improved the thermal insulation, mechanical and fire safety properties of materials while ensuring the light weight and degradability of aerogel composites (Fig. 1). Due to the existence of waxy layer on the surface of KF, it was firstly micro-treated and processed into 150~200 μm hollow tubular fibers by using unique cutting method to ensure the full component utilization of KF. PVA was used as a dispersing binder to ensure the high filling amount of KF, which made the aerogel construct a tubular-based 3D network structure. Moreover, with the introduction of flame retardant cross-linker BGP, the KF-PVA-BGP suspension exhibited a high viscosity at room temperature and thinning in shear (Fig. S1), which ensured that KF-PVA-BGP aerogel can be readily prepared by freeze-molding and -drying at any time. KF-PVA-BGP aerogel presents low shrinkage and high compressive strength due to their intermolecular interaction. This method uses recyclable and renewable bio-based KF as the matrix to prepare a novel biodegradable aerogel that integrates light weight, high strength, thermal insulation and fire safety, and the aerogel composite can be used as plant fertilizer during degradation process, which is in sharp contrast to non-degradable and unsustainable petrochemical-based plastics.

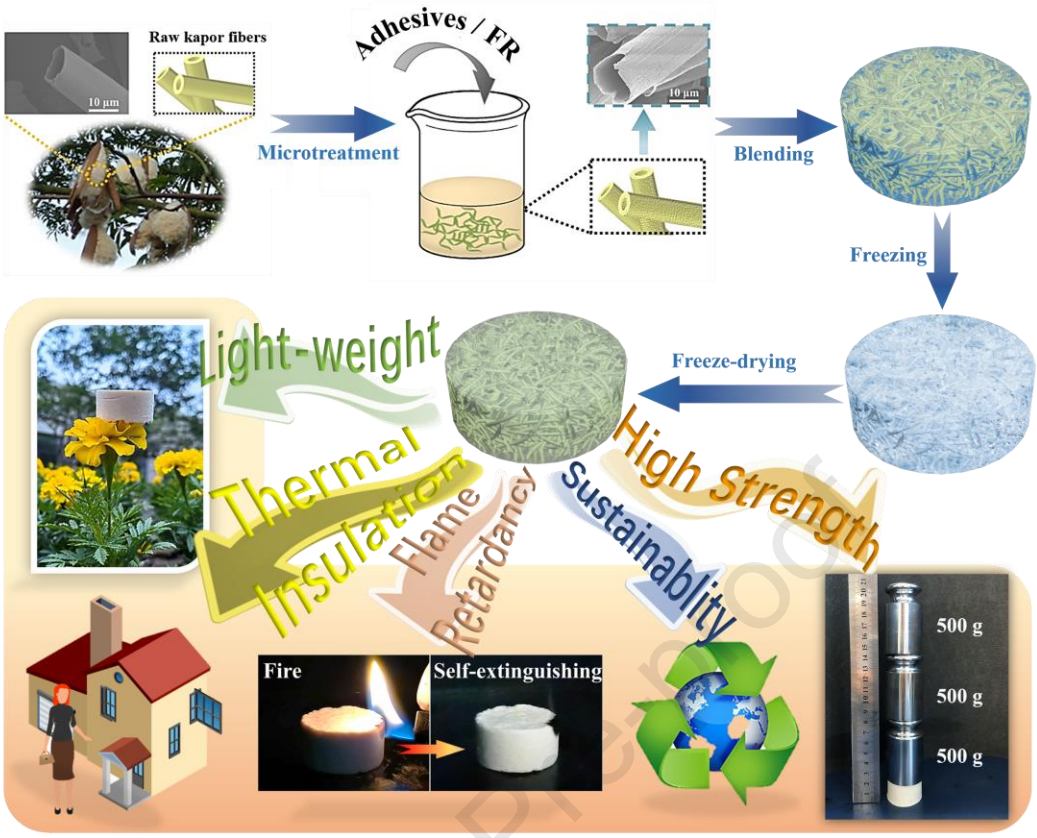

Fig. 1. Construction process and multifunctionality of KF aerogel composites.

2. Experimental Section

2.1. Materials

KF were supplied by Husheng Trading Co., Ltd. (Nanjing, China). NaOH was purchased from Fuchen Chemical Reagent Co., Ltd. (Shanghai, China). Both polyvinyl alcohol (PVA-1788) and biguanide phosphonate (BGP) were obtained from Aladdin Reagent Co., Ltd. (Shanghai, China).

2.2. Preparation of KF and flame retardant aerogels

First, the surface of KF was simply dewaxed with 8 g/L sodium hydroxide solution [31], and washed to pH=7. As shown in Fig. 1, the rough tube structure on KF surface was exposed. Then, the PVA is sequentially used in different proportions (1%, 2%, 3%, 4%, 5%, 6%, 7%) to rebuild the cross-linking network structure of KF. After freeze-drying at -60 °C for 72 h, KF aerogels were obtained. The prepared KF-PVA aerogels were named as KF, KF-PVA$_1$, KF-PVA$_2$, KF-PVA$_3$, KF-PVA$_4$, KF-PVA$_5$, KF-PVA$_6$, KF-PVA$_7$, respectively. Meanwhile, biguanide phosphonate (BGP) solutions with different concentrations were prepared according to the proportions of 2%, 4%, 6%, 8% and 10%, respectively, and then fully mixed with 5% KF-PVA solution to form

hydrogels. After freeze-drying at -60℃ for 72 h, flame retardant KF aerogels were obtained, which were named as KF-PVA_5-BGP_2, KF-PVA_5-BGP_4, KF-PVA_5-BGP_6, KF-PVA_5-BGP_8, KF-PVA_5-BGP_{10}, respectively.

2.3. Characterization

Scanning electron microscopy (JSM-7500F SEM, Japan) was used to collect the microstructures of the aerogels and char residue, and the EDS mapping was used to analyze element dispersion. Fourier transform infrared spectroscopy (FTIR) was recorded from 400 to 4000 cm^{-1} with a resolution of 4 cm^{-1} on Nicolet Avator 360 spectrometer (Madison, America). Solid-state ^{31}P NMR was analyzed on the AVANCE III HD-500 MHz spectrometer (Bruker, Germany). The C, N, O and P elements of aerogels and char residues were obtained from X-ray photoelectron spectrometer (XPS) (Thermofisher, America), and the thickness of XPS detection was about 10 nm. The porosity of KF aerogel was calculated from the apparent density (ρ) of the material according to equation 1. The a, b and c are percentages of KF, PVA and BGP, respectively.

$$porosity = \left(1 - \frac{\rho}{a \times \rho_{KF} + b \times \rho_{PVA} + c \times \rho_{BGP}}\right) \times 100\% \quad (1)$$

The mechanical performance was measured by universal testing machine (Shenzhen Reger Instrument Company, China). The thermal conductivity of aerogels was characterized by TPS 2500s Hot Disk Thermal Constant Analyzer (Sweden) at 25 ºC with a heating power of 20 mW and time of 40 s. Each specimen was tested at least 5 times, and the average value was used as the result. The thermographic images were obtained by a thermal imager of Testo 869 (Testo, Germany).

Cone calorimetry (CC) tests were performed on a cone calorimeter tester (West Sussex, UK) under the heat flux of 35 $kW \cdot m^{-2}$. The sample dimensions were 100 mm × 100 mm × 4 mm. Thermogravimetric analysis (TGA) was carried out on a STA 6000-SQ8 thermal analyzer with heating rate of 10 ºC·min^{-1} under nitrogen atmosphere. TG-IR of the samples was measured on the Perkin Elmer STA 4000-SP3 analyzer under the N_2 atmosphere and 10 mg of aerogel composites were heated to 800 ºC at 10 ºC·min^{-1}.

3. Results and discussion

3.1 Construction and microstructure of KF aerogels

In this research, multifunctional KF aerogels were successfully prepared by the method of mixing dispersion-freezing casting-lyophilized molding. First of all, in order to ensure the full utilization of KF, we only carried out a simple microtreatment to remove the wax on its surface. In Fig. S1, the waxy peaks of KF at 1741 and 1249 cm^{-1} disappeared obviously after alkali treatment and the aromatic groups in the structure were retained, which was beneficial to the application of KF with full composition and high value. The dewaxed KF can be uniformly dispersed with PVA and BGP in deionized water through mechanical stirring and the natural hollow KF was strongly bonded together due to the hydrogen bonding action between PVA, BGP and KF. Therefore, KF aerogels were endowed with excellent thermal insulation, flame retardancy and mechanical properties.

Fig. 2 showed the morphology of KF after treatment. KF was an obvious hollow structure with a diameter of approximately 15 μm (Fig. 2b). After alkali treatment, the surface of KF became rough due to the removal of wax, ash and water-soluble substances on the surface. In addition, the surface of treated KF possessed polyhydroxy structures and it can lap itself into an aerogel through freeze-forming and freeze-drying (Fig. 2b). However, the formed aerogel was easily broken and slag-dropped, and its volume shrinkage rate was relatively large, which cannot meet the needs of daily applications. With the introduction of binder PVA, the volume shrinkage of the KF-PVA aerogels were significantly decreased (Fig. S2). When the addition of PVA was 5 wt%, the volume retention rate of KF-PVA aerogel remained at approximately 91% and it basically did not change with the improvement of PVA content. The hollow structure of KF was obviously preserved with the introduction of PVA and the adhesion of treated KF was obviously improved (Fig. 2c). KF-PVA_5 aerogels exhibited the lowest density (0.0587 $g \cdot cm^{-3}$) due to its improved volume retention rate of KF-PVA aerogels and the 3D network structure between PVA and KF. After introducing BGP into KF-PVA_5 aerogels, the KF-PVA_5-BGP aerogels still maintained a low volume shrinkage (Fig. S2) and the porosity of KF-PVA_5-BGP aerogels was subsequently improved with the introduction of BGP (Fig. 2g). Meanwhile, because of the hydrogen bonding between BGP, PVA and KF, the adhesion between KF and PVA was stronger and the 3D network

structure was more obvious. It was beneficial for KF-PVA$_5$-BGP aerogels to obtain excellent mechanical and thermal insulation properties.

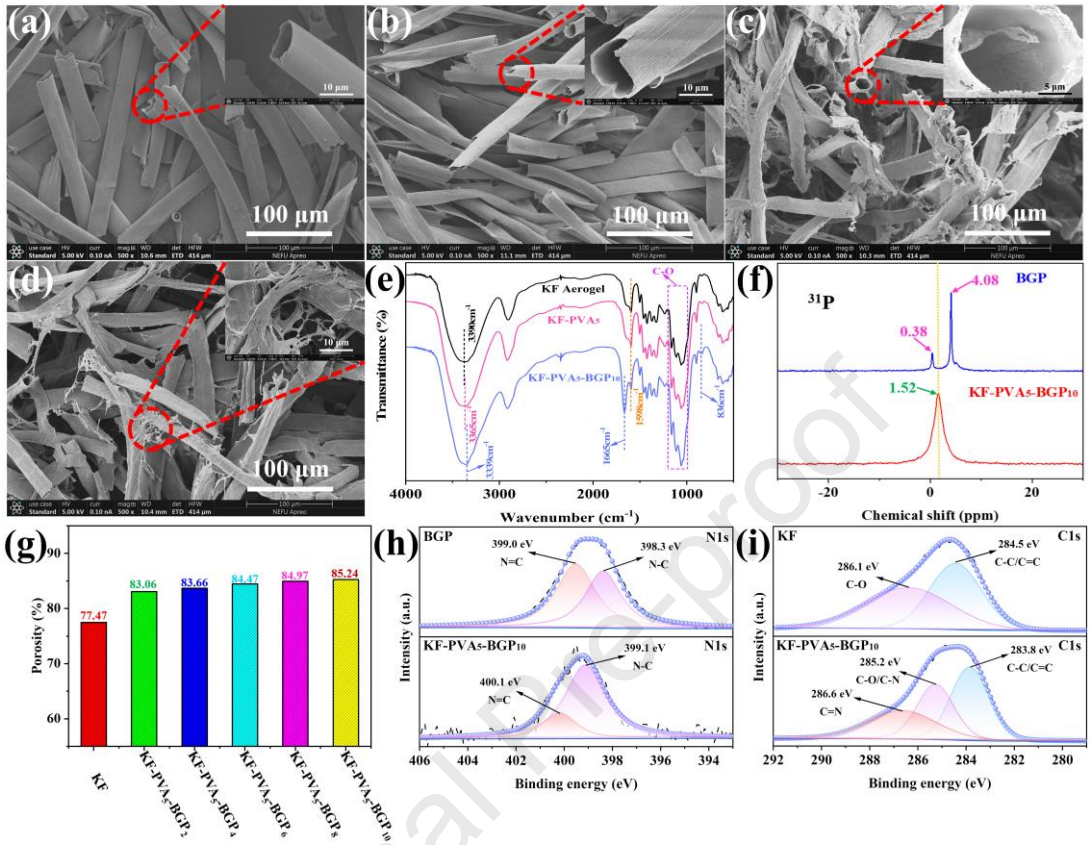

Fig. 2. SEM images of (a) untreated KF, (b) KF aerogel, (c) KF-PVA$_5$ and (d) KF-PVA$_5$-BGP$_{10}$ aerogels; (e) FTIR spectra of the KF, KF-PVA$_5$ and KF-PVA$_5$-BGP$_{10}$ aerogels; (f) ^{31}P solid-state NMR spectra of BGP and KF-PVA$_5$-BGP$_{10}$ aerogel; (g) Porosity of KF and KF-PVA-BGP aerogels; (h) High-resolution C1s XPS spectra of BGP and KF-PVA$_5$-BGP$_{10}$ aerogels; (i) High-resolution N1s XPS spectra of KF and KF-PVA$_5$-BGP$_{10}$ aerogel.

The FTIR, ^{31}P solid-state NMR and XPS spectra of KF, BGP, KF-PVA$_5$ and KF-PVA$_5$-BGP aerogels were shown in Fig. 2. The absorption peak of KF aerogel at 3390 cm^{-1} was attributed to the stretching vibration of -OH (Fig. 2e). The characteristic peak of aromatic structure at 1598 cm^{-1} indicated that lignin in KF was preserved after NaOH treatment. The absorption peaks at 1162, 1112 and 1056 cm^{-1} were ascribed to the stretching vibration of C-O in KF [31-33]. With the introduction of PVA and BGP, the stretching vibration peak of -OH gradually shifted to the lower band, which indicated the generation of hydrogen bonds between KF and PVA and BGP. Compared with KF and KF-PVA$_5$ aerogels, the new characteristic peak of C=N appeared at 1665 cm^{-1} in KF-PVA$_5$-BGP$_{10}$ and it demonstrated the successful doping of BGP. Meanwhile, the ^{31}P solid-state NMR of BGP indicated that its P chemical shift was 4.08 ppm and there was a small spike at 0.38 ppm due to the existence of a small amount of monophosphate in

BGP. When the BGP was introduced into the KF-PVA_5 aerogel matrix, the P chemical shift of BGP (1.52 ppm) obviously moved to the lower shifts due to the formation of hydrogen bonds. Besides, XPS data showed that the introduction of PVA and BGP increased the O, N and P content of KF aerogels. The C1s peaks of KF-PVA_5-BGP_{10} obviously detected C-N and C=N peaks at 285.2 and 286.6 eV compared with that of KF. The binding energy of N1s peaks (C-N and C=N) for KF-PVA_5-BGP_{10} were significantly higher than that of BGP (Fig. 2h). In Fig. S3, the P2p peaks combined with the above analysis further indicated the successful introduction of BGP and the role of intermolecular hydrogen bonding.

3.2 Mechanical performance and enhancement mechanism analysis

The KF aerogels can be tailored and processed into various complex shapes according to our requirements (Fig. 3d). Besides, the KF aerogels possessed a low density and can be stand on thin petals without deformation (Fig. 3c). Compared with traditional aerogels, KF-PVA-BGP aerogels not only ensured full-component and high-load utilization of biomass fiber resources, but also have high strength and low density [4,34]. The volume retention rate and mechanical resistance of KF-PVA aerogels were significantly enhanced compared with the friability and shrinkage of pure KF aerogel (Fig. S2 and 3d). When the introduction of PVA was 5 wt%, the mechanical strength of KF-PVA_5 aerogel exhibited the highest value (1.29 MPa). Meanwhile, the structure of KF-PVA aerogel was reinforced with the introduction of BGP and the compressive strength of KF-PVA_5-BGP_{10} was reached up to 1.64 MPa. 1 g specimen could withstand a mass 1500 times larger than itself without any deformation, which was relatively high in the reported organic aerogels (Fig. 3c) [35]. The improvement in strength for KF-PVA-BGP was attributed to the effect of their intermolecular hydrogen bonds and the corresponding enhancement mechanism was illustrated in Fig. 3e. PVA and BGP served as oxygen- and nitrogen-rich structures respectively and the introduction of N and O could generate hydrogen bonds with -OH groups on the surface of KF, leading to form the 3D network structure in aerogel and improving effectively their compression strength [36,37]. Secondly, although KF-PVA-BGP aerogels maintained a relatively low density, their density was slightly increased compared to KF-PVA aerogels, which was also positive for the enhancement of mechanical properties of KF-PVA-BGP aerogels.

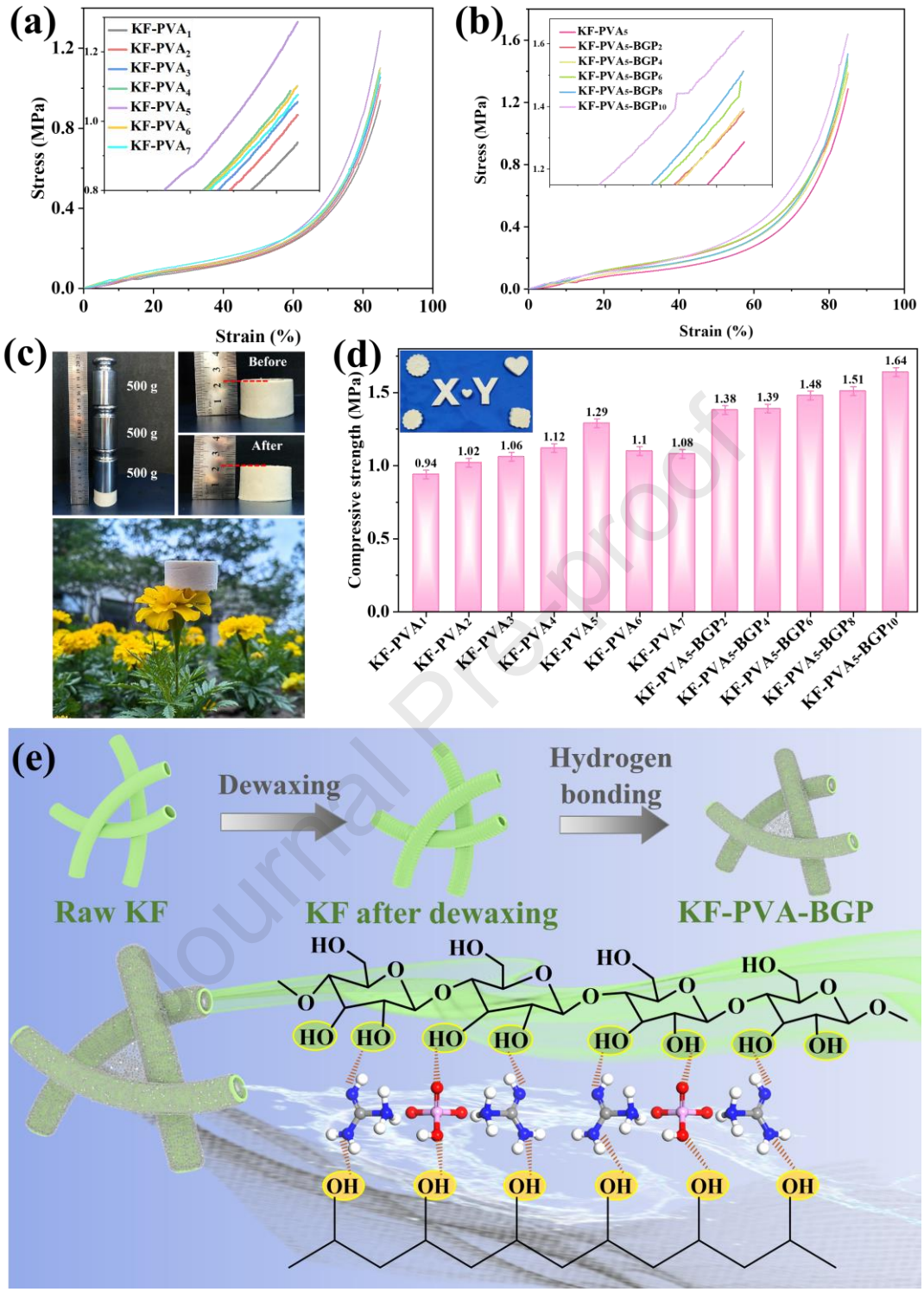

Fig. 3. Stress-strain curves of (a) KF-PVA and (b) flame retardant KF-PVA-BGP aerogels; (c) Images of KF-PVA$_5$-BGP$_{10}$ sample under the load of 1.5 kg without deformation; (d) Compressive strength of different KF aerogels and the various complex shapes of KF-PVA-BGP aerogels; (e) Schematic diagram of the mechanical enhancement mechanism of KF-PVA-BGP aerogels.

3.3 Thermal insulation analysis

Thermal insulation performance is an important indicator for the practical application of aerogel in the field of energy saving and thermal insulation. To study the

thermal insulation of high-strength aerogels constructed from natural hollow tubular fibers, the thermal conductivity and thermal images of KF aerogels at different temperatures were evaluated. The thermal conductivity of KF-PVA aerogels decreased gently due to the formation of 3D network structure in aerogels with the increase of PVA addition (Fig. 4a-b). The introduction of BGP made the hydrogen bond between KF and PVA strengthened, resulting in a slight increasement in the thermal conductivity of KF-PVA-BGP aerogel. But the KF-PVA-BGP aerogel still maintained a relatively low thermal conductivity and the thermal conductivity of KF-PVA$_5$-BGP$_{10}$ aerogel was only 0.0531 $W{\cdot}m^{-1}K^{-1}$, which was crucial for its use as thermal insulation materials in everyday life.

The infrared images of KF and KF-PVA$_5$-BGP$_{10}$ aerogel specimens at 50-200 ºC was used to further investigate their thermal insulation properties and the representative images and related data were shown in Fig. 4c-i. Compared with the lapped KF aerogel, the thermal insulation performance of KF-PVA$_5$-BGP$_{10}$ aerogel was significantly improved. When the stage temperature was heated to 200 ºC for 10 min, the ΔT of the KF-PVA$_5$-BGP$_{10}$ aerogels reached 125.4 ºC. In general, high ΔT values demonstrated the excellent thermal insulation properties of aerogels. Side view thermal images of KF and KF-PVA$_5$-BGP$_{10}$ aerogels were shown in Fig. 4c,d, when the hot stage temperature was maintained at 200 ºC for 10 min. The temperature of KF-PVA$_5$-BGP$_{10}$ was significantly lower than that of pure KF at the same height of aerogels. This was attributed to the improved volume retention and the construction of 3D networks for KF-PVA$_5$-BGP$_{10}$ aerogels.

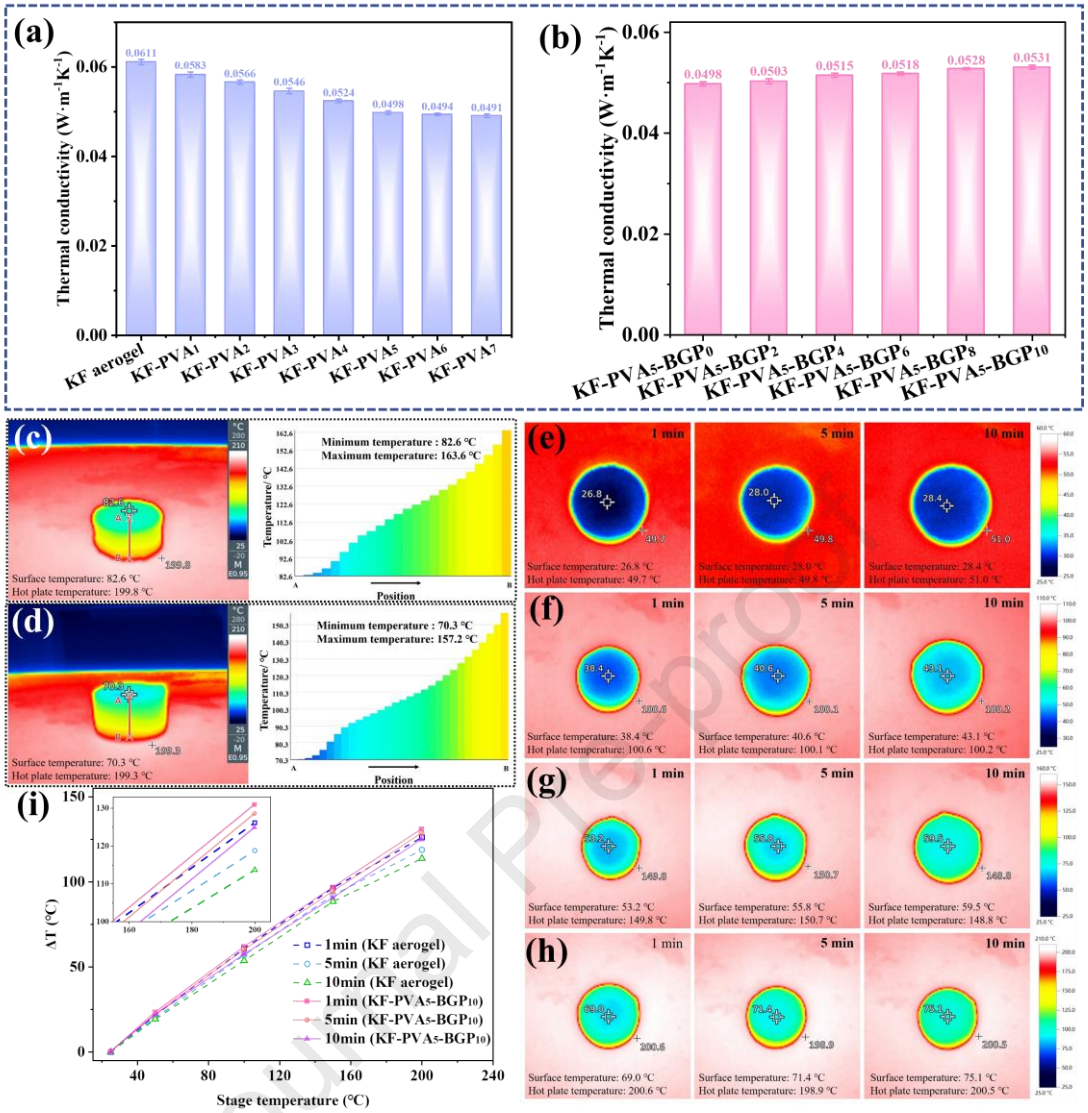

Fig. 4. Thermal conductivity diagram of (a) KF and (b) KF-PVA-BGP aerogel samples; Side view pseudo-color thermal image of (c) KF and (d) KF-PVA$_5$-BGP$_{10}$ aerogel with a height of 1.6 cm after heating at 200 ºC for 10min; Top side pseudo-color thermal images of the KF-PVA$_5$-BGP$_{10}$with a height of 1.6 cm after heating for 1, 5 and 10 min on a hot plate held at (e) 50 ºC, (f) 100 ºC, (g) 150 ºC and (h) 200 ºC; (i) Temperature difference (ΔT) curves between the surface of hot stage and KF-PVA$_5$-BGP$_{10}$.

3.4 Fire Hazard Analysis

The fire safety of organic aerogels is crucial in the field of energy saving and thermal insulation. Therefore, the flame retardancy of aerogels were evaluated by direct ignition method (ignite with a lighter for 1 s). Pure KF aerogel burned rapidly once it was near an ignition source and started to smolder after the open flame ended until it burned to a white flocculent ash (Fig. 5a). When the flammable binder PVA was introduced into the KF aerogels, the flammability of the KF-PVA$_5$ aerogels significantly increased and its burning time improved accordingly. In contrast, the KF-PVA$_5$-BGP$_{10}$ aerogels achieved a quick self-extinguishing effect with the introduction of BGP and

retained its original morphology after three ignitions. This possessed important implications for expanding the application value of high-strength organic KF aerogels.

In order to further analyze the effect of PVA and BGP on the combustion behaviour of KF aerogels, the cone calorimetry (CC) tests of KF, KF-PVA_5 and KF-PVA_5-BGP aerogels were performed and the related test data were shown in Fig. 5 and Table S1. Once pure KF aerogels was ignited, it showed a high PHRR (peak of heat release rate) value of 213.93 $kW \cdot m^{-2}$ and its THR (total heat release) was up to 19.21 $MJ \cdot m^{-2}$. The PHRR and THR of KF-PVA_5 aerogels were enhanced due to the introduction of flammable PVA. Interestingly, the introduction of flame retardant reinforcement BGP significantly reduced the PHRR and THR of KF-PVA_5 aerogels. When the introduction of BGP was only 10 wt%, the PHRR and THR of KF-PVA_5-BGP_{10} aerogels were decreased by 56.0% and 30.5%, respectively. This fact was mainly attributed that BGP promoted the cross-linking and charring of polyhydroxy KF-PVA matrix, which exerted the shielding effect in condensed phase. It was also evidenced by the early degradation and increased degradation rate of the aerogel composites in TG analysis of Fig. 5h-i.

In actual fires, the generation of smoke and toxic gases can easily lead to asphyxiation and they are more lethal than heat release. The PSPR (peak of smoke production rate) and TSP (total smoke production) of KF-PVA_5-BGP_{10} aerogels were decreased by 74.3% and 86.1% compared with those of KF aerogels (Fig. 5f-g). This significant decrease was ascribed to the excellent catalytic charring properties of BGP and the shielding effect of constituent char layer. It was also illustrated through the high residual mass in the TG analysis of Fig. 5h. In general, a high residual mass meant that less fuel was used for combustion. Thus, the KF-PVA-BGP aerogels showed excellent fire safety compared with traditional thermal insulation materials.

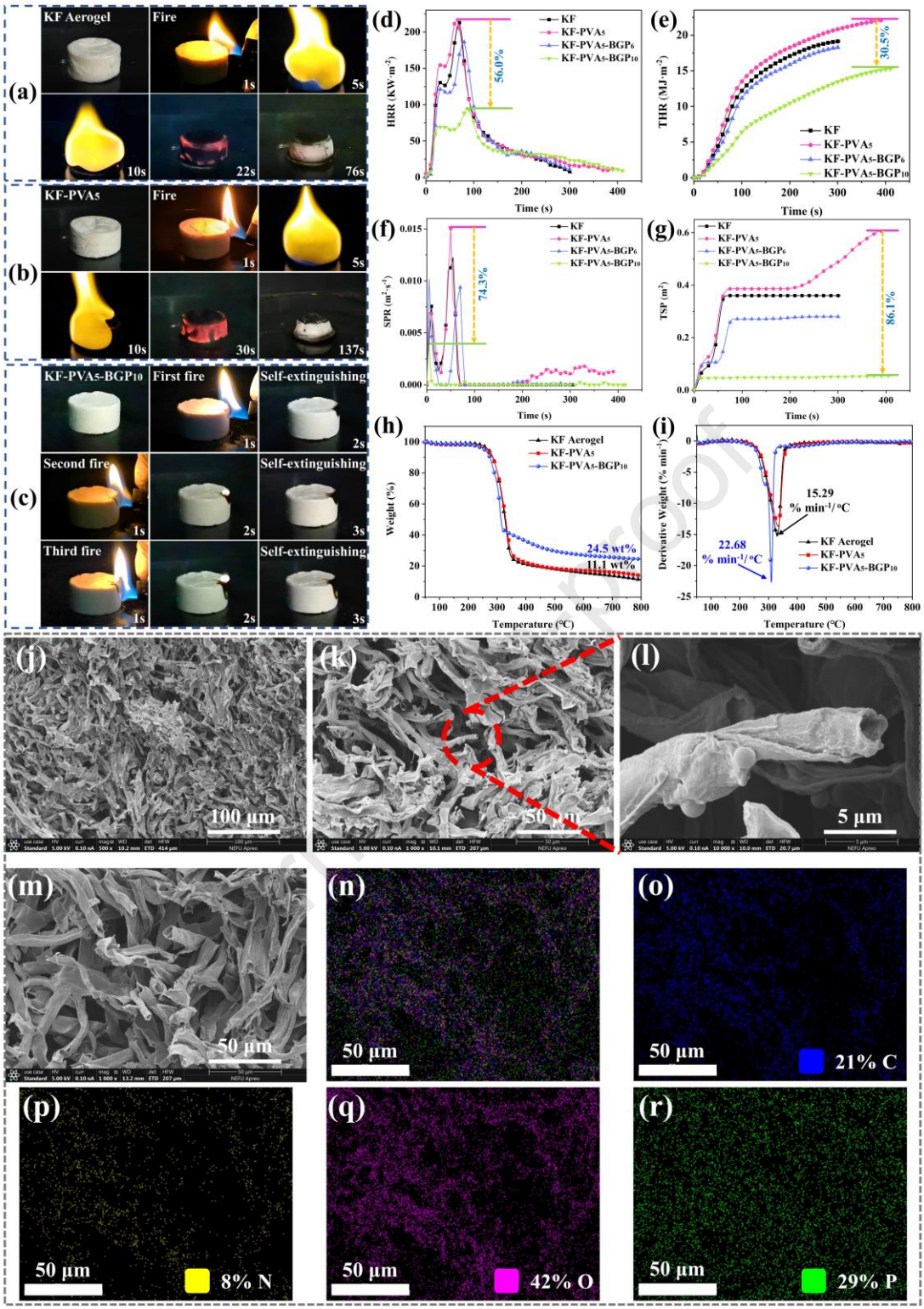

Fig. 5. Video screenshot of the combustion process of (a) KF, (b) KF-PVA_5 and (c) KF-PVA_5-BGP_{10} aerogels after ignition; (d) HRR, (e) THR, (f) SPR and (g) TSP curves of KF, KF-PVA_5, KF-PVA_5-BGP_6 and KF-PVA_5-BGP_{10} aerogels after CC tests; (h) TG and (i) DTG curves of KF, KF-PVA_5 and KF-PVA_5-BGP_{10} aerogels under N_2; (j-l) SEM images of residual char after CC tests for KF-PVA_5-BGP_{10} aerogels; (m) SEM image and (n-r) EDS Mapping of char residues for KF-PVA_5-BGP_{10} aerogels.

To make the fire hazard of aerogels clearer, their FPI (fire performance index), FGI (fire growth index) and FRI (flame retardancy index) was calculated according to

equations (2-4). Theoretically, flame retardant materials with a high FPI and low FGI demonstrated good fire safety. As shown in Table S1, the FPI value of KF-PVA-BGP aerogels increased and the FGI values decreased subsequently with the introduction of BGP addition, indicating that the fire hazard of KF-PVA-BGP aerogels was significantly reduced. Meanwhile, the FRI was used to evaluate the flame retardant performance of materials. The FRI of KF-PVA-BGP aerogels gradually increased with the introduction of BGP (Table S1). It meant that BGP efficaciously improved the flame retardant performance of aerogel composites. In summary, compared to conventional petrochemical-based energy saving and thermal insulation materials (e.g. polyurethane, polystyrene, etc.) [38], KF-PVA-BGP aerogels exhibited excellent fire safety performance in addition to their biodegradability. This novel aerogel materials possessed important research implications for reducing the risk to people and extending their escape and rescue time during a fire.

$$FPI = \frac{TTI}{PHRR} \tag{2}$$

$$FGI = \frac{PHRR}{T_{PHRR}} \tag{3}$$

$$FRI = \frac{\left[THR \times \left(\frac{PHRR}{TTI}\right)\right]_{Neat\ aerogel}}{\left[THR \times \left(\frac{PHRR}{TTI}\right)\right]_{Aerogel\ composites}} \tag{4}$$

3.5 Flame retardant mechanism analysis

The above fire hazard analysis indicated that KF-PVA-BGP aerogels exhibited excellent fire safety performance. In the following section, the flame retardant mechanism of KF-PVA-BGP aerogels was revealed through the combined gas- and condensed-phase analysis.

The photos, microscopic morphology and chemical structure composition of char residues for KF, KF-PVA$_5$ and KF-PVA-BGP aerogels after CC tests were shown in Fig. S4, 5 and 6. Pure KF and KF-PVA$_5$ only remained white flocculent residue under strong radiation. In Fig. 6a, FTIR analysis indicated that they were oxalic carbonates (υ_{CO3}:1448~1000 cm^{-1}, δ_{CO3}: 960~660 cm^{-1}) [39]. With the introduction of flame retardant enhancer BGP, the white grassy ash substance resembling KF aerogels disappeared obviously and the residual mass of KF-PVA-BGP aerogels was

significantly improved. When the introduction of BGP was 10 wt%, KF-PVA$_5$-BGP$_{10}$ aerogels formed a complete and coherent char layer after CC tests. The residual char of KF-PVA$_5$-BGP$_{10}$ aerogels had a compact and relatively dense morphological structure and retained the original hollow structure of KF after CC tests, which effectively acted as a heat shield and prevented the exchange of combustibles in condensed phase (Fig. 5j-l). The FTIR analysis of char residues for KF-PVA$_5$-BGP$_{10}$ exhibited several absorption peaks at 1592 cm^{-1} (aromatic ring), 1186 cm^{-1} (P=O) and 960 cm^{-1} (P-O), demonstrating the formation of a phosphorus-containing polyaryl char layer [40-42]. Meanwhile, EDS mapping and XPS analysis showed that the phosphorus-containing (13.14 wt%) compounds were homogeneously dispersed in condensed phase after CC tests. The BE (binding energy) peaks of O1s and P2p spectra for KF-PVA$_5$-BGP$_{10}$ proved the existence of O=P-O and PO$_3$ (Fig. 6 d,e). Combined with the BE peaks of C1s spectra, BGP produced pyro/polyphosphate during decomposition, which effectively promoted the generation of cross-linked char layers. This allowed KF to maintain its original tubular morphology and thus exerted an excellent shielding role in condensed phase.

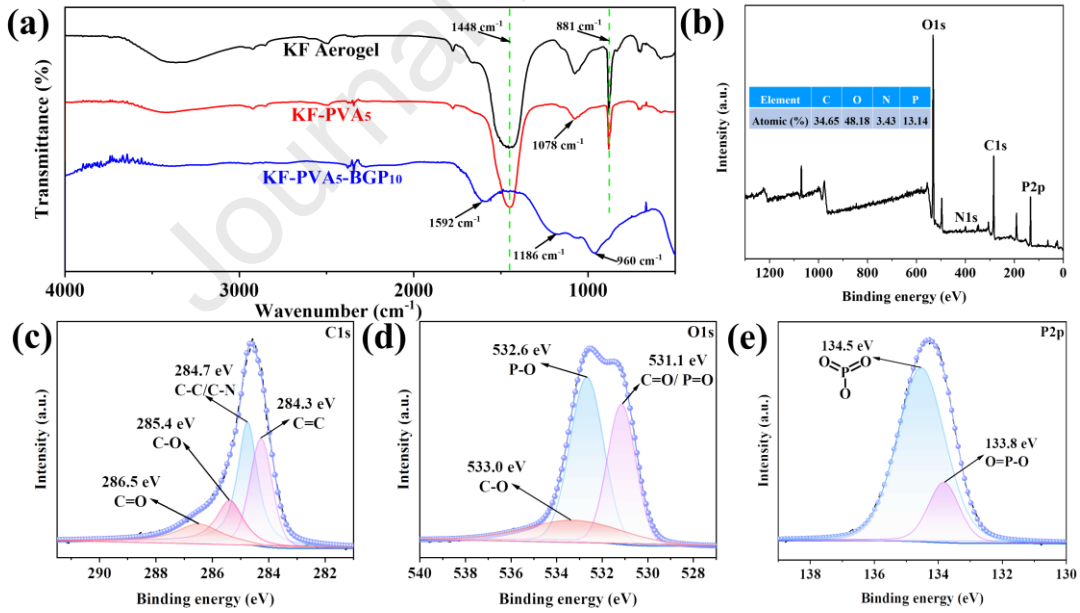

Fig. 6. (a) FTIR spectra of char residues for KF, KF-PVA$_5$ and KF-PVA$_5$-BGP$_{10}$ aerogels after CC tests; XPS (b) survey, (c) C1s, (d) O1s and (e) P2p spectra of residual char of KF-PVA$_5$-BGP$_{10}$ aerogel.

The real-time gaseous products directly affect the propagation and development of flame. Therefore, the pyrolysis products of KF, KF-PVA$_5$ and KF-PVA$_5$-BGP$_{10}$ aerogels were studied through TG-IR tests and their real-time results were shown in Fig. 7. The cellulose and most of lignin were retained after microtreatment of KF and

thus many typical pyrolysis products of KF aerogels mainly included water (3791, 3735 and 3567 cm^{-1}), hydrocarbons (2926 and 2898 cm^{-1}), CO_2 (2362 and 2322 cm^{-1}), CO (2182 and 2111 cm^{-1}), carbonyls (1744 cm^{-1}), aromatics (1508 cm^{-1}), ethers (1271 and 1105 cm^{-1}) [43-46]. When the polyhydroxyl binder PVA was introduced, the pyrolysis products of KF-PVA aerogels had no obvious change except for the increased absorption peak of water. Nevertheless, as shown in Fig. S5, the amount of pyrolysis products (especially hydrocarbons (2898 cm^{-1}), carbonyls (1744 cm^{-1}) and esters (1105 cm^{-1})) of KF-PVA-BGP was significantly lower than those of KF and KF-PVA aerogels with the introduction of BGP, which indicated that KF-PVA_5-BGP_{10} aerogels generated less flammable gas during thermal degradation, resulting a lower fuel feeding and decreasing the combustion process of aerogel composites. Meanwhile, the introduction of BGP promoted the dehydration and charring of KF-PVA aerogel in advance and thus KF-PVA_5-BGP_{10} aerogels produced a lot of water during their decomposition compared with KF, and the water and ammonia gas generated from the decomposition of BGP exerted the dilution effect in vapor phase. In addition, the catalytic carbonization of BGP resulted in relatively high content of aromatic compounds at the beginning of degradation, which was conducive to the formation of a hard and cross-linked high-quality char layers of KF-PVA-BGP aerogels. The shielding effect of char layer and the increase of residual mass significantly reduced the emission of toxic gas CO and effectively enhanced the smoke and toxicity suppression performance of organic aerogels.

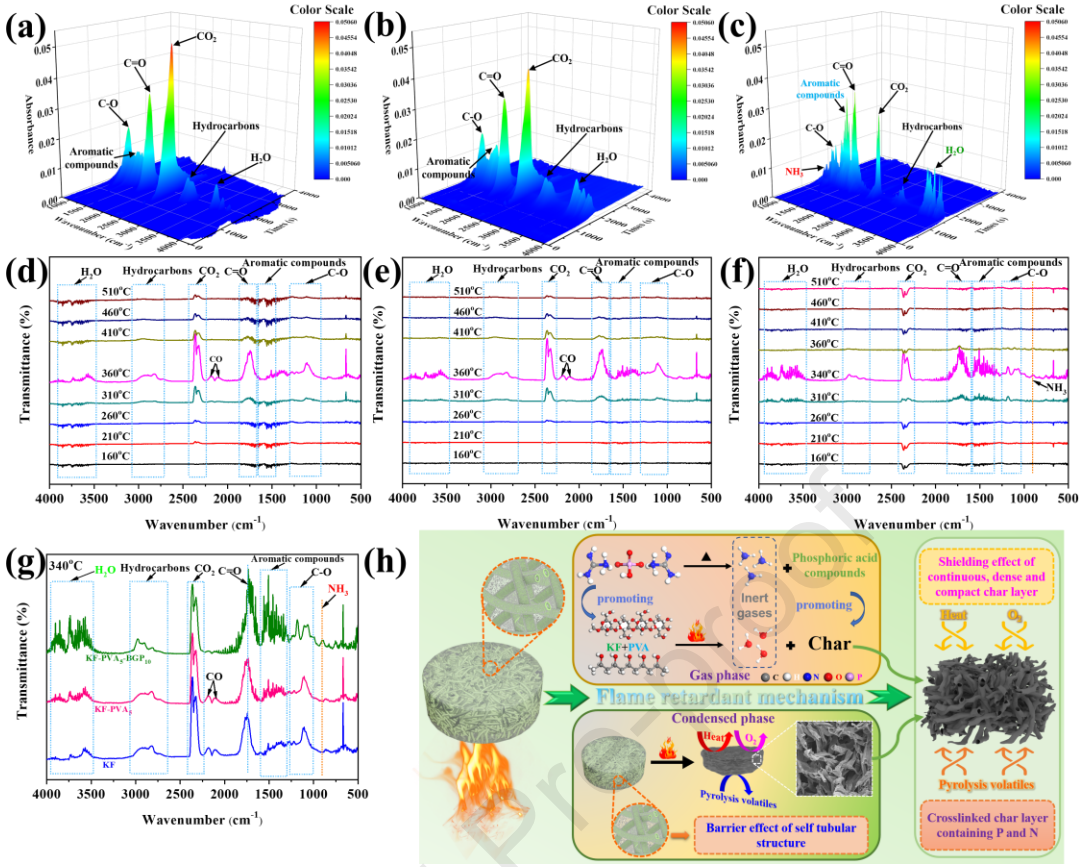

Fig. 7. 3D TG-FTIR spectra of pyrolysis products for (a) KF, (b) KF-PVA_5 and (c) KF-PVA_5-BGP_{10} aerogels; Time-dependent FTIR spectra of pyrolysis products for (d) KF, (e) KF-PVA_5 and (f) KF-PVA_5-BGP_{10} aerogels; (g) FTIR spectra of pyrolysis products for KF, KF-PVA_5 and KF-PVA_5-BGP_{10} aerogels at 340 °C; (h) Schematic diagram of the flame-retardant mechanism of KF-PVA-BGP aerogels.

Based on the above analysis, a possible flame retardant mechanism of KF-PVA-BGP was illustrated in Fig. 7h. Once the KF-PVA-BGP aerogels were burned, the decomposition of BGP produced phosphoric acid compounds, which promoted the dehydration and charring of the KF-PVA matrix. Ammonia and other non-combustible gases from the combustion of aerogel composites effectively exerted dilution role in gas phase, decreasing the burning intensity of aerogels. Meanwhile, KF-PVA-BGP aerogels formed a compact, homogeneous and dense tubular char layer, and its shielding effect with the aerogel itself prevented the exchange of heat, combustible volatiles and oxygen in condensed phase. Thus, KF-PVA-BGP aerogels presented excellent fire safety properties.

3.6 Multifunctional thermal insulation aerogels applied in cold conditions

In the application process, the actual insulation performance of energy conservation and heat shielding materials is very important. Currently, the commonly

used wall insulation materials in the markets are mainly petrochemical-based polystyrene (PS) boards. We prepared a simple house model by simulating the hot water heating conditions in the northern cold environment, and compared the thermal insulation performance of biodegradable KF-PVA_5-BGP_{10} aerogels and commercial PS boards (Fig. 8c). KF-PVA_5-BGP_{10} aerogels and PS foam possessed similar thermal insulation performance and the hot water could only drop to 30 ºC in 5 h compared with pure wooden buildings (Fig. 8e). Nevertheless, although the PS foam acquired in the market was treated with flame retardant, it was very easy to be ignited under strong ignition source and its combustion process generated a large amount of smoke, which caused asphyxiation and death of human beings during fire. Compared with commercial PS foam, KF-PVA_5-BGP_{10} bio-based aerogels not only has similar thermal insulation performance, but also exhibited excellent flame retardancy. KF-PVA_5-BGP_{10} was rapidly self-extinguishing under twice ignition of strong fire source, which was essential to enhance the fire safety performance of building insulation composites. Meanwhile, KF, as a light filling material, possessed good mildew resistance and it played a positive role on its use as a wall insulation material. Therefore, KF-PVA_5-BGP_{10} aerogels was successfully endowed with excellent thermal shielding, mechanical, flame retardant and smoke-suppression properties compared with traditional petrochemical-based PS boards by using its own hollow structure and 3D network construction while maintaining its biodegradability (Fig. 8h,i) [5]. This was a crucial support for the implementation of the global dual carbon strategy.

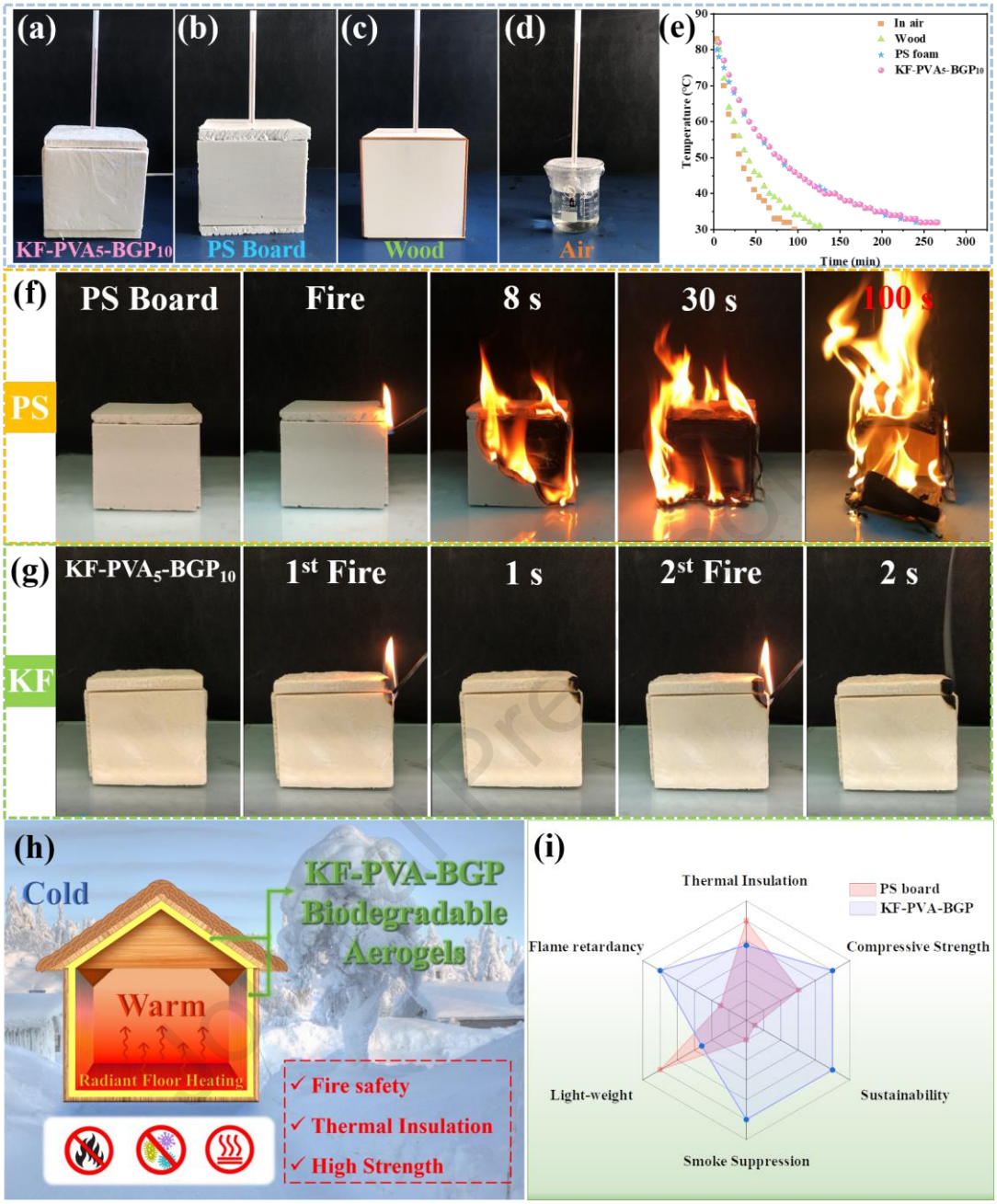

Fig. 8. Simulated small room built with (a) KF-PVA-BGP, (b) PS board, and (c) wood board, respectively; (d) Hydrothermal simulation of heating environment in northern cold region; (e) Curves of temperature change over time under KF-PVA-BGP insulation boards, PS boards, wood boards and air conditions; Comparison of burning video screenshot of model house built by commercial (f) PS boards and (g) KF-PVA-BGP insulation boards after ignition; (h) Illustrations of KF-PVA-BGP boards used for roofing, external wall panels and floor insulation materials of the energy-saving buildings; (i) Comparison of the comprehensive performance of KF-PVA-BGP aerogels and commercial PS boards by a radar chart.

4. Conclusions

In conclusion, we prepared a lightweight, insulating, robust, recyclable, biodegradable and excellent fire safety tubular aerogel with a 3D network structure by the now mature freeze-drying technique. KF-PVA-BGP suspensions possessed a high

apparent viscosity and KF-PVA-BGP aerogels can be manufactured easily, enabling high filling and high value utilization of bio-based KF. Compared with commercial PS insulation boards, the KF-PVA-BGP composites exhibited higher compression strength and excellent thermal insulation properties because of the construction of 3D network for tubular aerogels. Besides, BGP promoted the early degradation and charring of KF-PVA matrix and formed a tubular structured reinforced char layer, which effectively played the shielding effect in condensed phase. Therefore, KF-PVA-BGP composites exhibited excellent fire safety properties. Besides, KF-PVA-BGP aerogel had good recyclability and biodegradability compared with commercial insulation materials. This multifunctional recyclable bio-based aerogel has exhibited tremendous potential for application in emerging fields.

Acknowledgements

This work was financially supported by the National Key R&D Program of China (2022YFC3080600 and 2022YFC3003105), Natural Science Foundation of China (52203082), Fundamental Research Funds for the Central Universities (2572022BU02), Key Research and Development Projects in Heilongjiang Province (GZ20220056) and Undergraduate Innovation Project for Northeast Forestry University (202110225445). And the financial contributions from China Scholarship Council (202106600011) was also appreciated.

References

[1] Hauenstein O, Agarwal S, Greiner A. Bio-based polycarbonate as synthetic toolbox. Nat Commun 2016;7:11862.

[2] Rathore P, Gupta N, Yadav D, Shukla S, Kaul S. Thermal performance of the building envelope integrated with phase change material for thermal energy storage: an updated review. Sustain Cities Soc 2022;79:103690.

[3] Wu Y, Tan SJ, Zhao Y, Liang LL, Zhou M, Ji GB. Broadband multispectral compatible absorbers for radar, infrared and visible stealth application. Prog Mater Sci 2023;135:101088.

[4] Apostolopoulou-kalkavoura V, Munier P, Bergstrom L. Thermally insulating nanocellulose-based materials. Adv Mater 2021;33:2001839.

[5] Yang Z, Li H, Niu G, Wang J, Zhu D. Poly(vinylalcohol)/chitosan-based high-strength, fire-retardant and smoke-suppressant composite aerogels incorporating aluminum species via freeze drying. Compos Part B-Eng 2021;219:108919.

[6] Gu WH, Shen YH, Guo WY, Fang YT, Ji GB, Xu ZC. A lightweight, elastic, and thermally insulating stealth foam with high infrared-radar compatibility. Adv Sci 2022;9(35):2204165.

[7] Liu L, Feng JB, Xue YJ, Chevali V, Zhang YB, Shi YQ, Tang LC, Song PA. 2D MXenes for fire retardancy and fire-warning applications: promises and prospects. Adv Funct Mater 2023;33(9):2212124.

[8] Yan W, Shen Y, An W, Jiang L, Zhou Y, Sun J. Experimental study on the width and pressure effect on the horizontal flame spread of insulation material. Int J Therm Sci 2017;114:114-22.

[9] Wang K, Fu C, Wang R, Tao G, Xia Z. High-resilience cotton base yarn for anti-wrinkle and durable heat-insulation fabric. Compos Part B-Eng 2021;212:108663.

[10] Kuranska M, J. Pinto A, Salach K. Synthesis of thermal insulating polyurethane foams from lignin and rapeseed based polyols: A comparative study. Ind Crop Prod 2020;143:111882.

[11] Wang Y, Liu J, Zhao Y, Qin Y, Zhu Z, Yu Z, He H. Temperature-triggered fire warning PEG@wood powder/carbon nanotube/calcium alginate composite aerogel and the application for firefighting clothing. Compos Part B-Eng 2022;247:110348.

[12] Chen X, Zhou M, Zhao Y. Morphology control of eco-friendly chitosan-derived carbon aerogels for efficient microwave absorption at thin thickness and thermal stealth. Green Chem 2022;24:5280-90.

[13] Lou G, Ma Z, Dai J, Bai Z, Fu S, Huo S, Qian L, Song PA. Fully biobased surface-functionalized microcrystalline cellulose via green self-assembly toward fire-retardant, strong, and tough epoxy biocomposites. ACS Sustainable Chem Eng 2021;40:13595-13605.

[14] Chen W, Yu H, Lee S. Nanocellulose: a promising nanomaterial for advanced electrochemical energy storage. Chem Soc Rev 2018;47:2837-72.

[15] Chen Y, Zhang L, Yang Y. Recent Progress on Nanocellulose Aerogels: Preparation, Modification, Composite Fabrication, Applications. Adv Mater 2021;33:2005569.

[16] Gu P, Liu W, Hou Q. Lignocellulose-derived hydrogel/aerogel-based flexible quasi-solid-state supercapacitors with high-performance: a review. J Mater Chem A. 2021;9:14233-64.

[17] Hu F, Wu S, Sun Y. Hollow-structured materials for thermal insulation. Adv Mater 2019;31:1801001.

[18] Wicklein B, Kocjan A, Salazar-alvarez G. Thermally insulating and fire-retardant lightweight anisotropic foams based on nanocellulose and graphene oxide. Nat Nanotechnol 2015;10:277-83.

[19] Dong T, Tian N, Xu B, Huang X, Chi S, Liu Y, Lou C, Lin J. Biomass poplar catkin fiber-based superhydrophobic aerogel with tubular-lamellar interweaved neurons-like structure. J Hazard Mater 2022;429:128290.

[20] Thilagavathi G, Karan C, Das D. Oil sorption and retention capacities of thermally-bonded hybrid nonwovens prepared from cotton, kapok, milkweed and polypropylene fibers. J Environ Manage 2018;219:340-9.

[21] Wang J, Zheng Y, Wang A. Coated kapok fiber for removal of spilled oil. Mar Pollut Bull 2013;69:91-6.

[22] Mu P, Bai W, Fan Y. Conductive hollow kapok fiber-PPy monolithic aerogels with excellent mechanical robustness for efficient solar steam generation. J Mater Chem A 2019;7:9673-9.

[23] Xiang H, Wang D, Liu H. Investigation on sound absorption properties of kapok fibers. Chinese J Polym Sci 2013;31:521-9.

[24] Ahankari S, Paliwal P, Subhedar A. Recent developments in nanocellulose-based aerogels in thermal applications: A review. ACS Nano 2021;15:3849-74.

[25] Zhang S, Li S, Wu Q, Li Q. Phosphorus containing group and lignin toward intrinsically flame retardant cellulose nanofibril-based film with enhanced mechanical properties. Compos Part B-Eng 2021;212:108699.

[26] Han Y, Zhang X, Wu X. Flame Retardant, Heat insulating cellulose aerogels from

waste cotton fabrics by in situ formation of magnesium hydroxide nanoparticles in cellulose gel nanostructures. ACS Sustain Chem Eng 2015;3:1853-9.

[27] Koklukaya O, Carosio F, Wagberg L. Superior Flame-resistant cellulose nanofibril aerogels modified with hybrid layer-by-layer coatings. ACS Appl Mater Inter 2017;9:29082-92.

[28] Yang W, Ping P, Wang L. Fabrication of fully bio-based aerogels via microcrystalline cellulose and hydroxyapatite nanorods with highly effective flame-retardant properties. ACS Appl Nano Mater 2018;1:1921-31.

[29] Gupta P, Verma C, Maji P. Flame retardant and thermally insulating clay based aerogel facilitated by cellulose nanofibers. J Supercrit Fluid 2019;152:104537.

[30] Zhao S, Malfait W, Demilecamps A, Zhang Y, Brunner S. Strong, Thermally superinsulating biopolymer-silica aerogel hybrids by cogelation of silicic acid with pectin. Angew Chem Int Ed 2015;127:14490-14494.

[31] Zhou M, Wang JW, Wang GH, Zhao Y, Tang JM, Pan JX, Ji GB. Lotus leaf-inspired and multifunctional Janus carbon felt@ Ag composites enabled by in situ asymmetric modification for electromagnetic protection and low-voltage joule heating. Compos Part B-Eng 2022;242(1):110110.

[32] Zong E, Wang C, Yang J, Zhu H, Jiang S, Liu X, Song PA. Preparation of TiO_2/cellulose nanocomposites as antibacterial bio-adsorbents for effective phosphate removal from aqueous medium. Int J Biol Macromol 2021;182:434-444.

[33] Khan F, Wang S, Ma Z, Ahmed A, Song PA, Xu Z. A durable, flexible, large-area, flame-retardant, early fire warning sensor with built-in patterned electrodes. Small Methods 2021;5:2001040.

[34] Yeo S, Oh M, Yoo P. Structurally controlled cellular architectures for high-performance ultra-lightweight materials. Adv Mater 2019;31:1803670.

[35] Aoudi B, Y Boluk, Eldin M. Recent advances and future perspective on nanocellulose-based materials in diverse water treatment applications. Sci Total Environ 2022;843:156903.

[36] Liu L, Xu XD, Zhu MH, Cui XH, Feng JB, Rad ZF, Wang H, Song PA. Bioinspired

strong, tough, and biodegradable poly (vinyl alcohol) and its applications as substrates for humidity sensors. Adv Mater Technol 2023;8(7):2201414.

[37] Liu L, Zhu M, Xu XD, Li X, Ma ZW, Jiang Z, Pich A, Wang H, Song PA. Dynamic nanoconfinement enabled highly stretchable and supratough polymeric materials with desirable healability and biocompatibility. Adv Mater 2021;33(51):2105829.

[38] Muhammed R, Hambali H, Khan Z. Emerging trends in flame retardancy of rigid polyurethane foam and its composites: A review. J Cell Plast 2022;59:65-122.

[39] Wang S, Dai G, Yang H. Lignocellulosic biomass pyrolysis mechanism: A state-of-the-art review. Prog Energ Combust 2017;62:33-86.

[40] Liu L, Zhu MH, Ma ZW, Xu XD, Seraji SM, Yu B, Sun ZQ, Wang H, Song PA. A reactive copper-organophosphate-MXene heterostructure enabled antibacterial, self-extinguishing and mechanically robust polymer nanocomposites. Chem Eng J 2022;430(1):132712.

[41] Liu L, Xu Y, Xu M, Li B. Facile synthesis of an efficient phosphonamide flame retardant for simultaneous enhancement of fire safety and crystallization rate of poly (lactic acid). Chem Eng J 2021;421:127761.

[42] Jia C, Zhang P, Seraji S, Xie R, Chen L, Liu D, Xiong Y, Chen H, Fu Y, Xu H, Song PA. Effects of BN/GO on the recyclable, healable and thermal conductivity properties of ENR/PLA thermoplastic vulcanizates. Compos Part A Appl Sci Manuf 2022;152:106686.

[43] Liu L, Xu Y, Xu M, Li B. Economical and facile synthesis of a highly efficient flame retardant for simultaneous improvement of fire retardancy, smoke suppression and moisture resistance of epoxy resins. Compos Part B-Eng 2019;167:422-433.

[44] Xu X, Li L, Seraji S, Liu L, Jiang Z, Xu Z, Li X, Zhao S, Wang H, Song PA. Bioinspired, strong and tough nanostructured poly(vinyl alcohol)/inositol composites: How hydrogen-bond cross-linking works? Macromolecules 2021;50(20):9510-9521.

[45] Huang QQ, Zhao Y, Wu Y, Zhou M, Tan SJ, Tang SL, Ji GB. A dual-band transceiver with excellent heat insulation property for microwave absorption and low infrared emissivity compatibility. Chem Eng J 2022;446(4):137279.

[46] Liu C, Zhang T, Luo Y, Wang Y, Li J, Ye T, Guo R, Song PA, Zhou J, Wang H. Multifunctional polyurethane sponge coatings with excellent flame retardant, antibacterial, compressible, and recyclable properties. Compos Part B-Eng 2021;125:108785.

Highlights

- A 3D network structure of tubular aerogel was successfully constructed by the now mature freeze-drying technique.

- KF-PVA-BGP aerogels exhibited high strength and thermal insulation properties due to intermolecular hydrogen bonding.

- Compared to commercial petrochemical-based insulation materials, KF-PVA-BGP aerogels possessed excellent fire safety properties while maintaining its biodegradability and recyclability.

- BGP exerted its flame-retardant effect in KF aerogels through the synergistic effect of gas and condensed phase.

Declaration of Competing Interest

The authors declare that they have no known competing financial interests or personal relationships that could have appeared to influence the work reported in this paper.

Credit Author Statement：

Yue Xu: Methodology, Conceptualization; Data curation; Formal analysis; Investigation, Writing-original draft, Writing - review & editing. Chentao Yan: Conceptualization, Investigation. Chunlin Du: Investigation. Kai Xu: Methodology. Yixuan Li: Data curation; Formal analysis. Miaojun Xu: Methodology, Project administration, Conceptualization, Investigation, Review-editing. Serge Bourbigot: Investigation, Conceptualization. Gaelle Fontaine: Methodology, Investigation. Bin Li: Funding acquisition, Supervision, Investigation, Resources, Funding acquisition; Lubin Liu: Formal analysis; Project administration, Investigation, Writing-original draft, Writing - review & editing.